NANO LETTERS

Letter

pubs.acs.org/NanoLett

# Giant Mechanocaloric Effects in Fluorite-Structured Superionic Materials

Claudio Cazorla*[,†,‡] and Daniel Errandonea[§]

[†]School of Materials Science and Engineering and [‡]Australia Integrated Materials Design Centre, University of New South Wales Australia, Sydney New South Wales 2052, Australia

[§]Departamento de Física Aplicada (ICMUV), Malta Consolider Team, Universitat de Valencia, 46100 Burjassot, Spain

Supporting Information

**ABSTRACT:** Mechanocaloric materials experience a change in temperature when a mechanical stress is applied on them adiabatically. Thus, far, only ferroelectrics and superelastic metallic alloys have been considered as potential mechanocaloric compounds to be exploited in solid-state cooling applications. Here we show that giant mechanocaloric effects occur in hitherto overlooked fast ion conductors (FIC), a class of multicomponent materials in which above a critical temperature, $T_s$, a constituent ionic species undergoes a sudden increase in mobility. Using first-principles and molecular dynamics simulations, we found that the superionic transition in fluorite-structured FIC, which is characterized by a large entropy increase of the order of $10^2$ $JK^{-1}$ $kg^{-1}$, can be externally tuned with hydrostatic, biaxial, or uniaxial stresses. In particular, $T_s$ can be reduced several hundreds of degrees through the application of moderate tensile stresses due to the concomitant drop in the formation energy of Frenkel pair defects. We predict that the adiabatic temperature change in $CaF_2$ and $PbF_2$, two archetypal fluorite-structured FIC, close to their critical points are of the order of $10^2$ and $10^1$ K, respectively. This work advocates that FIC constitute a new family of mechanocaloric materials showing great promise for prospective solid-state refrigeration applications.

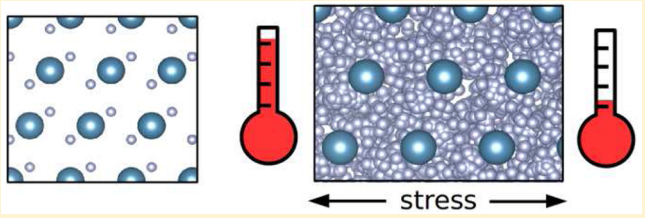


**KEYWORDS:** *Fast-ion conductor, solid-state cooling, density functional theory, molecular dynamics*

Fast-ion conductors (FIC) are solids in which ions are highly mobile. They are usually employed as electrolytes in solid-state batteries.[1,2] Above a certain critical temperature, $T_s$, the anion or cation mobility in FIC becomes comparable to that of a molten salt, namely of the order of 1 $\Omega^{-1}cm^{-1}$. This "superionic" transition can be thought of as a sublattice melting that, in analogy to homogeneous melting, has associated a large increase in entropy and lattice parameter.[3,4] $CaF_2$ is an archetypal FIC that under ambient conditions crystallizes in the cubic fluorite structure (space group $Fm\bar{3}m$). In this compound, the critical temperature for $F^-$ diffusivity is 1400 (90) K and the accompanying raise in entropy 225.6 $JK^{-1}$ $kg^{-1}$.[5,6] The accepted dominant effect behind the large ionic conductivity observed in $CaF_2$ and other analogous FIC is the formation of Frenkel pair defects (FPD), that is, the simultaneous creation of $F^-$ vacancies and interstitials.[7,8]

Recently, it has been demonstrated by state-of-the-art compression experiments and first-principles calculations that the superionic temperature in $CaF_2$ can be largely modified with the application of hydrostatic pressure. For instance, $T_s$ increases as much as ∼200 K under a homogeneous load of 5 GPa.[5] This fundamental finding suggests that external mechanical stress, $\sigma$, could be used to control the superionic transition in FIC, a possibility that, due to the huge entropy change associated with the transformation and structural simplicity and abundance of the involved materials, could be highly exploitable in energy conversion applications. However, a thorough understanding of the atomic mechanisms mediating the observed stress-induced $T_s$ variation is still lacking, and thus possible scientific and technological developments are being hampered. Here, we apply a fully atomistic simulation approach to fill this critical knowledge gap. In particular, we rationalize how the critical temperature in fluorite-structured FIC is affected by compressive ($\sigma > 0$) and tensile ($\sigma < 0$) hydrostatic, biaxial, and uniaxial stresses and evaluate the potential of this effect for solid-state cooling operation.

Three types of mechanical stress were considered in our study: hydrostatic ($\sigma_{xx} = \sigma_{yy} = \sigma_{zz}$), biaxial ($\sigma_{xx} = \sigma_{yy}$, $\sigma_{zz} = 0$), and uniaxial ($\sigma_{xx} = \sigma_{yy} = 0$, $\sigma_{zz}$). We adopted a rigid-ion Born–Mayer–Huggins (BMH) interatomic potential to describe the interactions between atoms in $CaF_2$.[9,10] This interaction potential renders a satisfactory description of $T_s$ under varying hydrostatic stress, as it is demonstrated in Figure 1a through the comparison to first-principles results obtained with density functional theory (DFT) [for technical details, see Supporting Information]. At equilibrium ($\sigma = 0$), the adopted BMH potential provides a superionic critical temperature of 1350 (50) K, which is in good accordance with reported experimental data and DFT calculations.[5] In view of such an agreement, we assume that the classical BMH and first-

**Received:** January 31, 2016
**Revised:** April 6, 2016
**Published:** April 12, 2016





DOI: 10.1021/acs.nanolett.6b00422
*Nano Lett.* 2016, 16, 3124–3129

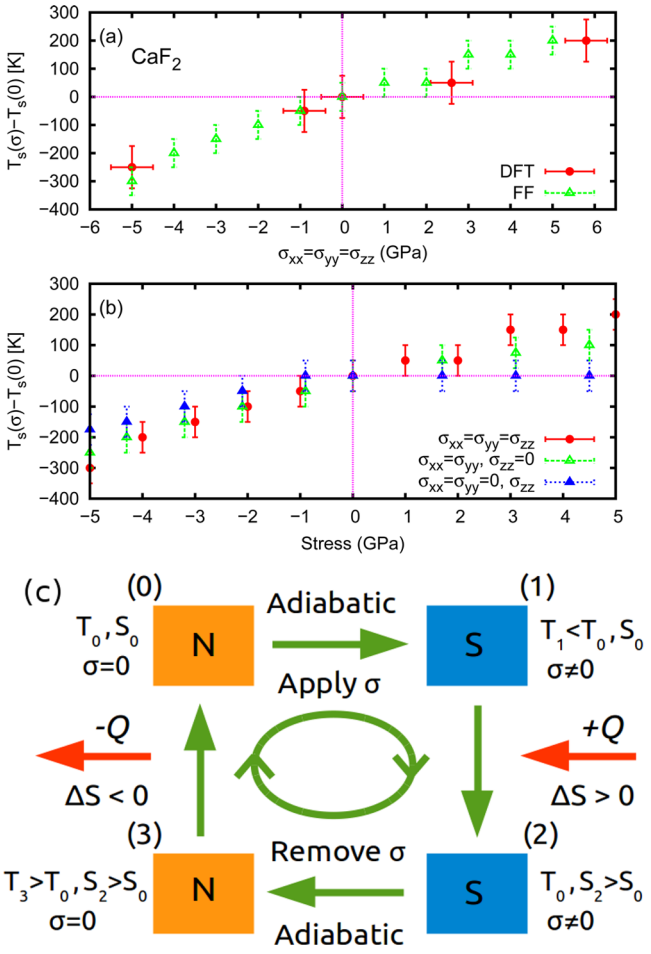


**Figure 1.** (a) The superionic temperature in $CaF_2$ expressed as a function of hydrostatic stress and calculated with first-principles (DFT) and molecular dynamics (FF) simulation methods. (b) Critical superionic temperature expressed as a function of hydrostatic, biaxial, and uniaxial stresses, calculated with molecular dynamics simulation methods. (c) Schematic representation of a mechanocaloric cooling cycle based on a fluorite-structured FIC at $T_0 < T_s(0)$ . "N" and "S" represent the normal and superionic states. (0) → (1) A tensile stress is applied adiabatically triggering superionicity and thus the crystal gets cooler. (1) → (2) The crystal receives heat from a system and thus $T$ and $S$ increase. (2) → (3) The external stress is removed adiabatically and thus the crystal reverts to the normal state and $T$ increases. (3) → (4) Heat is ejected to the environment.

principles DFT results obtained in the rest of cases are also consistent.

Figure 1b shows the stress dependence of $T_s$ calculated under broad $\sigma > 0$ (compressive) and $\sigma < 0$ (tensile) stress conditions. At compressive stress, the superionic features in $CaF_2$ rely markedly on the type of $\sigma$ that is applied. For instance, in the hydrostatic case $T_s$ increases as much as ∼200 K under a maximum load of 5 GPa, whereas the same critical temperature remains practically insensitive to uniaxial compressive stresses of the same magnitude. The results obtained for biaxial compressive stresses shows a tendency that is kind of an average between the hydrostatic and uniaxial cases. Under $\sigma < 0$ stress conditions, however, all three types of stresses produce similar effects on $T_s$ and superionicity emerges at temperatures significantly lower than at equilibrium. For instance, at the maximum tensile load considered here $T_s$ is reduced as much as 200−300 K.

In view of the $T_s(\sigma)$ results presented in Figure 1b, one can think of many original mechanocaloric cooling cycles involving FIC. Among all the possibilities, we sketch in Figure 1c one consisting of two adiabatic (that is, constant entropy) and two constant uniaxial $\sigma < 0$ steps. The change in temperature occurring during the two adiabatic processes is

$$\Delta T = -\int_0^{|\sigma_f|} \frac{T}{C_\sigma} \mathrm{d}S = -\int_0^{|\sigma_f|} \frac{T}{\rho_0 C_\sigma} \left(\frac{\partial \epsilon}{\partial T}\right)_\sigma \mathrm{d}\sigma \qquad (1)$$

where $\rho_0$, $C_\sigma$, and $\epsilon$ represent the equilibrium density, heat capacity, and mechanical strain, respectively, in the FIC. The operation temperature for such an hypothetical refrigeration cycle is $T < T_s(0)$, that is, the FIC is initialized from the nonsuperionic (or normal) state. Upon application (removal) of tensile stress the entropy of the crystal increases (decreases) due to triggering (prevention) of the superionic state, thereby its temperature decreases (increases) [that is, $\Delta S > 0$ implies $\Delta T < 0$ and vice versa, see eq 1]. We note that the represented cooling sequence works in "inverse" order to usual refrigeration cycles based on ferroelectrics and shape-memory alloys.[11−14] The reason for this is that the state of maximum entropy is accessed through the switching-on of the external field. (We note than an "inverse" electrocaloric effect has been proposed recently in ferroelectrics by Ponomareva and Lisenkov;[15] this consists in applying an electric field orthogonal to the ferroelectric polarization in order to induce disordering of the dipoles and thus an increase in the entropy.) Nonetheless, the normal cycling operation can always be recovered by setting $T > T_s(0)$ and applying compressive stresses instead.

In order to rationalize the physical origins of the $T_s(\sigma)$ results shown in Figure 1, we computed the formation energy of Frenkel pair defects (FPD) for all considered stresses with first-principles DFT methods (see Figure 2). For this, we constructed a cubic supercell containing 144 atoms that subsequently was relaxed according to the imposed $\sigma$-conditions. Structural phase tranformations other than the $Fm\bar{3}m \rightarrow I4/mmm$ transition, which naturally occurs in the uniaxial and biaxial cases (see Supporting Information), were absent in our geometry optimizations. An arbitrary $F^-$ ion then was moved away from its equilibrium position according to the Cartesian displacement $(u, v, w)$, where $0 \leq u, v, w \leq \frac{a_i}{2}$ and $\{a_i\}$ are the lattice parameters of the corresponding unit cell. The three Cartesian directions were sampled with 5 equidistant starting points (that is, a total of 125 relaxations were performed in each case). We systematically found that the only metastable interstitial configuration associated with the fluorine ion was $\left(\frac{a_x}{2}, \frac{a_y}{2}, \frac{a_z}{2}\right)$, which ordinarily is known as the octahedral site. As it is shown in Figures 2a,b, this configuration became also unstable (that is, the $F^-$ ion returned to its equilibrium lattice site during the relaxation) under moderate uniaxial and biaxial compressive stresses, probably due to the loss of crystal symmetry as compared to the hydrostatic case. We note that even though other interstitial positions are likely to be stabilized by effect of temperature,[2,16] we disregarded thermal excitations in this part of our study.

Our results in Figure 2 show that the overall effect of applying compressive stress in $CaF_2$ is to increase the formation energy of FPD, thereby hindering superionicity. On the contrary, tensile stress clearly enhances $F^-$ mobility by depleting the corresponding migration energy barrier. The variation of the FPD formation energy behaves linearly with


DOI: 10.1021/acs.nanolett.6b00422
Nano Lett. 2016, 16, 3124−3129

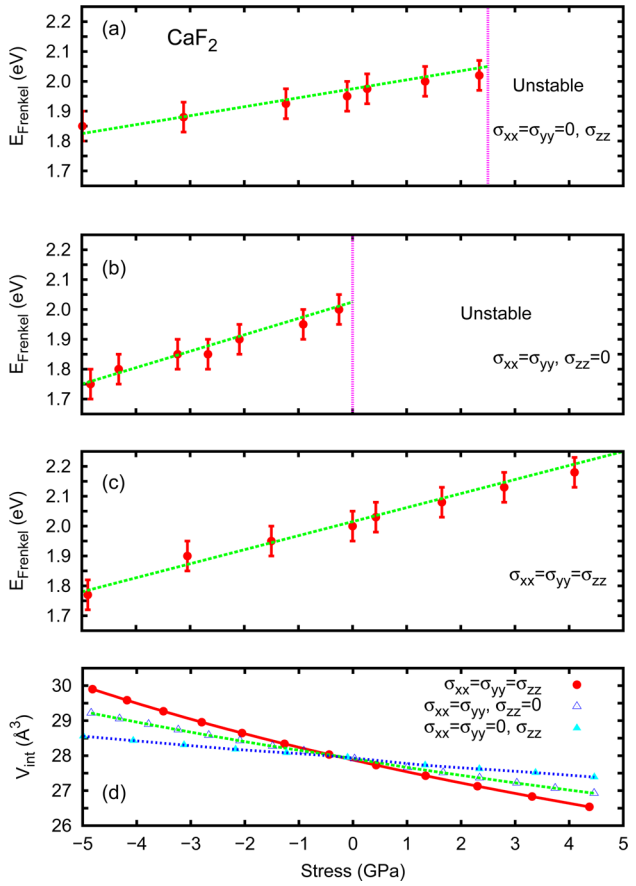


**Figure 2.** Formation energy of Frenkel pair defects in $CaF_2$ calculated with first-principles DFT methods and expressed as a function of uniaxial (a), biaxial (b), and hydrostatic (c) stress. "Unstable" indicates that during relaxation of the crystal the $F^-$ interstial returned to its equilibrium lattice position. (d) Available volume to the interstitial expressed as a function of stress.

respect to the external stress and is not bounded from below. These trends are correlated with the variation of volume that is available to the fluorine interstitial, $V_{int}$, which is defined as the empty octahedron space embedded in the perfect fluorite structure (see Figure 2d).[2,16] This volume expands or reduces roughly in proportion to $\sigma$, depending on whether the applied stress is tensile or compressive. In analogy to $T_s$, hydrostatic stress induces the largest $V_{int}$ variation whereas uniaxial stress induces the smallest. The larger $V_{int}$ is, the smaller the FPD formation energy results are. These structural and migration energy barrier outcomes clarify the causes behind the $T_s(\sigma)$ trends shown in Figure 1, confirming hydrostatic and biaxial stresses as most effective for tuning of the transport properties in FIC. Our findings may have an immediate application to the nanodesign of energy conversion devices with improved performance, as the results of recent experimental studies on microsolid oxide fuel cells appear to indicate;[17,18] however, for the sake of focus we will not elaborate on this aspect here.

It is worth noting that in practice tensile stress can be achieved both in the uniaxial and biaxial cases, and that $CaF_2$ can be deposited as a thin film on different substrates.[19−21] Tensile stresses are induced by the in-plane lattice mismatch between $CaF_2$ and the substrate, when the latter has a larger lattice parameter. According to our first-principles DFT calculations, $\sigma_{xx} = \sigma_{yy} = -5$ GPa conditions, for instance, correspond to an epitaxial strain of $\eta = +2.8\%$ (where $\eta \equiv a - a_0/a_0$ and $a_0 = 5.52$ Å). In this regard, Germanium appears to be a good candidate substrate because it is structurally compatible with $CaF_2$ and has a lattice parameter of ∼5.7 Å.

In order to assess the potential of fluorite-structured FIC for prospective solid-state cooling applications, we calculated the adiabatic temperature change induced on $CaF_2$ by the application of tensile stress, $\Delta T$, with molecular dynamics simulations (i.e., using the BMH interaction model). To this end, we computed the isothermal entropy change associated with each type of stress, $\Delta S$, and heat capacity of the crystal as a function of $T$ and $\sigma$, and subsequently integrated them according to eq 1 or an equivalent expression[22] (for technical details, see Supporting Information). It is important to stress that the only approximations affecting our results are all referred to the BMH potential, which otherwise has been demonstrated to be accurate enough for present purposes. Neither phenomenological models nor experimental data were assumed in our calculations.

The computed $\Delta S$ and $\Delta T$ considering a maximum tensile stress of 5 GPa and temperatures $T_s(0) - 300\ \text{K} \le T \le T_s(0)$ are shown in Figure 3. The results obtained in the three $\sigma$-cases are qualitatively very similar. At $\sigma = 0$ conditions, for example, both the isothermal entropy and adiabatic temperature changes are practically null. This applies even to the highest analyzed temperature because we identified $T_s$ with the onset of $F^-$ diffusivity, rather than with the peak in the heat capacity that appears at higher $T$ when superionicity is fully developed[3,4] (see Supporting Information). As tensile stress is raised, both $\Delta S$ and $\Delta T$ steadily increase in absolute value and their variation becomes larger at higher temperatures. As a consequence, no stationary points were found in our adiabatic or isothermal calculations in consistency with the findings shown in Figure 2. From a quantitative point of view, the results obtained in the hydrostatic and biaxial cases are both comparable and superior in terms of mechanocaloric potential to those found for uniaxial stresses. For instance, at $T = 1350$ K and considering $\sigma = -5$ GPa, the adiabatic temperature change (istohermal entropy change) calculated in the hydrostatic, biaxial, and uniaxial cases are ∼−152 (186), −163 (200), and −38 K (46 $JK^{-1}\ kg^{-1}$), respectively.

The mechanocaloric results just presented reveal that fluorite-structured FIC are auspicious materials for solid-state refrigeration. Although the involved temperatures are well above ambient conditions and the considered tensile stresses are moderately large, considering FIC in cooling applications may result in several advantages with respect to usual ferroelastic and ferroic materials. First, the predicted $\Delta T$ and $\Delta S$ are about 1 order of magnitude larger than (hydrostatic case) or comparable to (uniaxial case) the benchmark results reported thus far.[22,23] Second, the analyzed normal → superionic transition is of second-order type, and in contrast to ferroic materials, for example, FIC do not present order-parameter domains. These features are highly desirable for improved cyclability and rate capability of likely cooling devices, because thermal and mechanical hysteresis effects deriving from irreversible processes then would be smallest.[14,24] Actually, recent ultrafast X-ray spectroscopy experiments have demonstrated that the characteristic time scale of superionic switching is of the order of few picoseconds.[25] Third, the predicted $\Delta T$ and $\Delta S$ exhibit a uninterrupted escalation with respect to tensile stress (see Figure 2). This means that one could virtually go down to the ideal tensile strength of the crystal, which corresponds to its mechanical instability limit, in order to


DOI: 10.1021/acs.nanolett.6b00422
Nano Lett. 2016, 16, 3124−3129

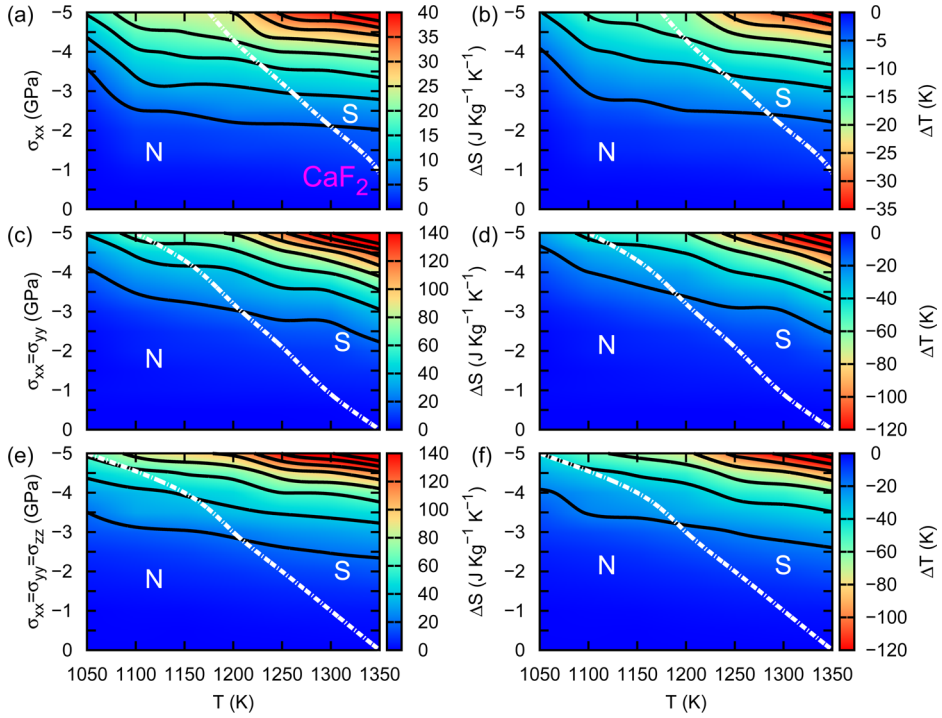


**Figure 3.** Isothermal entropy, $\Delta S$, and adiabatic temperature, $\Delta T$, changes in $CaF_2$ calculated with molecular dynamics simulation techniques and expressed a function of stress and temperature. Results enclosed in (a,b) correspond to uniaxial stress, (c,d) to biaxial, and (e,f) to hydrostatic. "N" and "S" represent the normal and superionic states and the thick dashed lines mark their corresponding phase boundaries.

maximally lower $T_s$ and augment $|\Delta T|$. We note that in ferroelectric−paraelectric or austenite−martensite transformations the resulting adiabatic temperature changes inevitably start decreasing beyond a certain threshold value of the external field due to saturation of the involved order parameters.[12,13]

It is well-known that the critical temperature in superionic materials can be reduced significantly by means of nanopatterning and chemical substitution strategies.[2,26] Aimed at alleviating the technical shortcomings found in $CaF_2$, we investigated the same class of superionic and mechanocaloric phenomena in $PbF_2$, a related fluorite-structured FIC with a much lower transition temperature of $T_s(0) \sim 700$ K.[27] (We note that by minimally doping $PbF_2$ with potassium ions it is possible to reduce the corresponding critical temperature practically down to ambient conditions.[28]) We adopted a rigid-ion BMH interatomic potential to describe the interactions between atoms in $PbF_2$.[29] This interaction potential also renders a satisfactory description of $T_s$ under varying hydrostatic stress, as it is demonstrated in Figure 4a through the comparison to first-principles DFT results. At equilibrium the adopted BMH potential provides a superionic critical temperature of 650(50) K, which is in good agreement with the experiments and DFT calculations.

The calculated $T_s(\sigma)$ trends in $PbF_2$ under hydrostatic and biaxial stresses are qualitatively analogous to those found in $CaF_2$ (see Figure 4a,b). Namely, tensile stress effectively depletes the corresponding critical temperature whereas compressive stress increases it. Also, the energy barrier for $F^-$ migration decreases roughly in proportion to the tensile stress and is not disrupted from below (see Figure 4c). We note that in our classical BMH and first-principles DFT simulations it was not possible to reproduce hydrostatic stress conditions below ∼−3 GPa due to the appearance of mechanical instabilities in the system. We tentatively identify this stress

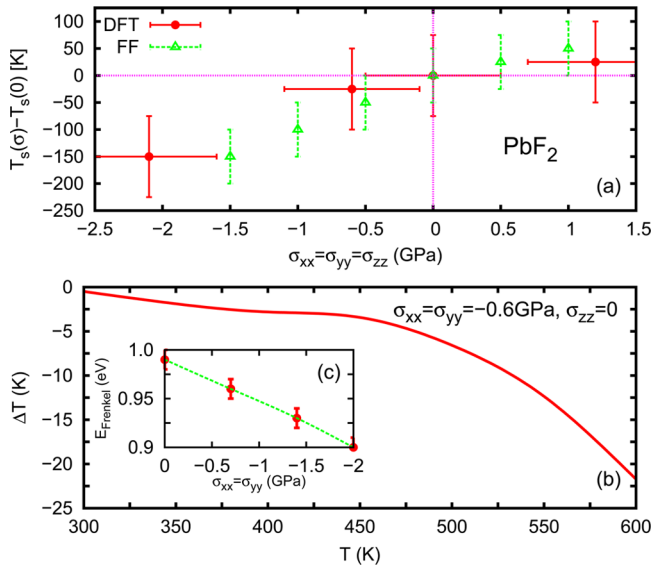


**Figure 4.** (a) The superionic temperature in $PbF_2$ expressed as a function of hydrostatic stress and calculated with first-principles (DFT) and molecular dynamics (FF) simulation methods. (b) Adiabatic temperature change, $\Delta T$, calculated in $PbF_2$ with molecular dynamics simulation methods and expressed as a function of temperature. The applied biaxial tensile stress is −0.6 GPa. (c) Formation energy of Frenkel pair defects in $PbF_2$ calculated with first-principles DFT methods and expressed as a function of biaxial tensile stress.

threshold with the ideal tensile strength in $PbF_2$ (a similar mechanically unstable regime was accessed also in $CaF_2$ but at $\sigma < -6$ GPa). At the quantitave level, we found two main differences between the two investigated FIC. First, smaller stresses are needed in $PbF_2$ to achieve a same critical



DOI: 10.1021/acs.nanolett.6b00422
Nano Lett. 2016, 16, 3124−3129

temperature reduction. For example, a $T_s(\sigma) - T_s(0)$ difference of −150 K is produced by a hydrostatic stress of $\sigma \sim -1.5$ GPa in $PbF_2$ and of $\sim -3.0$ GPa in $CaF_2$. Second, when considering a same tensile stress the adiabatic temperature change calculated close to the critical point is larger (in absolute value) in $PbF_2$. For instance, at $\sigma_{xx} = \sigma_{yy} = -0.6$ GPa the estimated $\Delta T$ in $PbF_2$ is ∼−20 K (see Figure 4b) and in $CaF_2$ is ∼− 2 K (see Figure 3d). This finding can be rationalized in terms of the accompanying isothermal entropy changes, which for small $\sigma$ are much larger in $PbF_2$. Finally, we note that according to our first-principles DFT calculations a tensile stress of, for example, ∼− 0.5 GPa is realizable in $PbF_2$ thin films through a small epitaxial strain of $\eta = +0.5\%$ (where $a_0$ = 6.03 Å). Switching back and forth from zero to moderate tensile stresses is actually possible in thin films by means of elastic bending techniques,[30] mechanical nanojigs,[31] or the use of piezoelectric substrates,[32] as it has been experimentally demonstrated in magnetic oxide compounds. Hence, the results just explained indicate that $PbF_2$ is a promising material for near-room-temperature cooling applications.

In summary, we have employed classical molecular dynamics and first-principles DFT simulation techniques to discern the relations between external mechanical stress and ionic transport in fluorite-structured FIC. Our computational study shows that hydrostatic, biaxial, and uniaxial stresses can be used as effective means for tuning of the critical temperature in superionic compounds. This finding may have also important implications for the design of solid-state batteries with improved ion diffusion kinetics. We have predicted that the adiabatic temperature change occurring in fluorite-structured FIC under external tensile stress is comparable in magnitude to current benchmark results reported for ferroelastic and ferroic materials. Our conclusions for $CaF_2$ and $PbF_2$ could be generalized to other FIC like, for instance, $Ag^+$ chalcogenides and halides and Li-based complex hydrides, with critical temperatures closer to room temperature. The present work therefore opens a new and promising avenue for the rational design of original refrigeration materials.

**Methods.** *Classical and DFT Computer Simulations.* Molecular dynamics ($N$, $P$, $T$) simulations were performed with the LAMMPS code.[33] The pressure and temperature in the system were kept fluctuating around a set-point value by using thermostatting and barostatting techniques in which some dynamic variables are coupled to the particle velocities and simulation box dimensions. Large simulation boxes containing 6144 atoms were used and periodic boundary conditions were applied along the three Cartesian directions. Newton's equations of motion were integrated using the customary Verlet's algorithm with a time-step length of $10^{-3}$ ps. A particle−particle particle−mesh $k$-space solver was used to compute long-range van der Waals and Coulomb interactions and forces beyond a cutoff distance of 12 Å at each time step.

First-principles DFT calculations were performed with the VASP code,[34] following the generalized gradient approximation to the exchange-correlation energy due to Perdew.[35] The "projector augmented wave" method was used to represent the ionic cores,[36] and the electronic states 2s-3s-3p-4s of Ca, 5d-6s-6p of Pb, and 2s-2p of F were considered as valence. Wave functions were represented in a plane-wave basis truncated at 500 eV. By using these parameters and dense $k$-point grids for Brillouin zone integration, the resulting enthalpies were converged to within 1 meV per formula unit. In the geometry relaxations, a tolerance of 0.01 eV·Å$^{-1}$ was imposed in the atomic forces. Further details of our classical and ab initio molecular dynamics simulations can be found in the Supporting Information.

## ■ ASSOCIATED CONTENT

### Supporting Information

The Supporting Information is available free of charge on the ACS Publications website at DOI: 10.1021/acs.nanolett.6b00422.

Additional details of the classical molecular dynamics and density functional theory calculations performed in $CaF_2$ and $PbF_2$ under hydrostatic, biaxial, and uniaxial stress conditions are provided. Special emphasis is put on the computation of the isothermal entropy, $\Delta S$, and adiabatic temperature, $\Delta T$, changes induced by varying stresses. The structural and energy results calculated with first-principles methods in both fluorite-structured superionic materials and the heat capacity and strain curves obtained with classical molecular dynamics are also reported. (PDF)

## ■ AUTHOR INFORMATION


### Corresponding Author

*E-mail: c.cazorla@unsw.edu.au.


### Author Contributions

All authors contributed equally to the present work.

### Notes

The authors declare no competing financial interest.

## ■ ACKNOWLEDGMENTS


This research was supported under the Australian Research Council's Future Fellowship funding scheme (Project Number FT140100135). Computational resources and technical assistance were provided by the Australian Government through Magnus under the National Computational Merit Allocation Scheme. D.E. acknowledges financial support from Spanish MINECO under Grants MAT2013-46649-C04-01 and MAT2015-71070-REDC (MALTA Consolider).


## ■ REFERENCES


(1) Hayes, W.; Stoneham, A. M. *Defects and Defect Processes in Non-metallic Solids*; Wiley: New York, 1985.

(2) Hull, S. Superionics: crystal structures and conduction processes. *Rep. Prog. Phys.* **2004**, *67*, 1233−1314.

(3) Andersen, N. H.; Clausen, K.; Kjems, J. K. Heavily doped $M_1U_xF_{2+2x}$ fluorites studied by quasielastic neutron scattering (M = Ba) and specific heat measurements (M = Pb). *Solid State Ionics* **1983**, *9-10*, 543−548.

(4) Goff, J. P.; Hayes, W.; Hull, S.; Hutchings, M. T. Neutron powder diffraction study of the fast-ion transition and specific heat anomaly in $\beta$-lead fluoride. *J. Phys.: Condens. Matter* **1991**, *3*, 3677−3687.

(5) Cazorla, C.; Errandonea, D. Superionicity and Polymorphism in Calcium Fluoride at High Pressure. *Phys. Rev. Lett.* **2014**, *113*, 235902−5.

(6) Ubbelohde, A. R. *The Molten State of Matter*; Wiley: New York, 1978.

(7) Gillan, M. J. Collective dynamics in superionic $CaF_2$: I. Simulation compared with neutron-scattering experiment. *J. Phys. C: Solid State Phys.* **1986**, *19*, 3391−3411; Dynamics of defects in superionic fluorites. *J. Chem. Soc., Faraday Trans.* **1990**, *86*, 1177−1182.

(8) Lindan, P. J. D.; Gillan, M. J. Shell-model molecular dynamics simulation of superionic conduction in $CaF_2$. *J. Phys.: Condens. Matter* **1993**, *5*, 1019−1030.




DOI: 10.1021/acs.nanolett.6b00422
*Nano Lett.* 2016, 16, 3124−3129

(9) Cazorla, C.; Errandonea, D. High-Pressure, High-Temperature Phase Diagram of Calcium Fluoride from Classical Atomistic Simulations. *J. Phys. Chem. C* **2013**, *117*, 11292−11301.
(10) Cazorla, C. In the search of new electrocaloric materials: Fast ion conductors. *Results Phys.* **2015**, *5*, 262−263.
(11) Scott, J. F. Electrocaloric Materials. *Annu. Rev. Mater. Res.* **2011**, *41*, 229−240.
(12) Liu, Y.; Wei, J.; Janolin, P.-E.; Infante, I. C.; Kreisel, J.; Lou, X.; Dkhil, B. Prediction of giant elastocaloric strength and stress-mediated electrocaloric effect in $BaTiO_3$ single crystals. *Phys. Rev. B: Condens. Matter Mater. Phys.* **2014**, *90*, 104107−6.
(13) Tuśek, J.; Engelbrecht, K.; Millán-Solsona, R.; Mañosa, L.; Vives, E.; Mikkelsen, L. P.; Pryds, N. The Elastocaloric Effect: A Way to Cool Efficiently. *Adv. Energy Mater.* **2015**, *5*, 1500361−5.
(14) Tuśek, J.; Engelbrecht, K.; Mikkelsen, L. P.; Pryds, N. Elastocaloric effect of Ni-Ti wire for application in a cooling device. *J. Appl. Phys.* **2015**, *117*, 124901−11.
(15) Ponomareva, I.; Lisenkov, S. Bridging the Macroscopic and Atomistic Descriptions of the Electrocaloric Effect. *Phys. Rev. Lett.* **2012**, *108*, 167604−5.
(16) Castiglione, M. J.; Madden, P. A. Fluoride ion disorder and clustering in superionic $PbF_2$. *J. Phys.: Condens. Matter* **2001**, *13*, 9963−9983.
(17) Shi, Y.; Bork, A. H.; Schweiger, S.; Rupp, J. L. M. The effect of mechanical twisting on oxygen ionic transport in solid-state energy conversion membranes. *Nat. Mater.* **2015**, *14*, 721−727.
(18) Fluri, A.; Pergolesi, D.; Roddatis, V.; Wokaun, A.; Lippert, T. In situ stress observation in oxide films and how tensile stress influences oxygen ion conduction. *Nat. Commun.* **2016**, *7*, 10692−9.
(19) Maki, T.; Okamoto, K.; Sugiura, M.; Hosomi, T.; Kobayashi, T. The great improvement of surface smoothness of $CaF_2$ in pulsed laser deposition even under the two-photon absorption process. *Appl. Surf. Sci.* **2002**, *197-198*, 448−451.
(20) Pilvi, T.; Arstila, K.; Leskelä, M.; Ritala, M. Novel ALD Process for Depositing $CaF_2$ Thin Films. *Chem. Mater.* **2007**, *19*, 3387−3392.
(21) Pandey, R. K.; Kumar, M.; Khan, S. A.; Kumar, T.; Tripathi, A.; Avasthi, D. K.; Pandey, A. C. Study of electronic sputtering of $CaF_2$ thin films. *Appl. Surf. Sci.* **2014**, *289*, 77−80.
(22) Moya, X.; Kar-Narayan, S.; Mathur, N. D. Caloric materials near ferroic phase transitions. *Nat. Mater.* **2014**, *13*, 439−450.
(23) Mañosa, L.; Planes, A.; Acet, M. Advanced materials for solid-state refrigeration. *J. Mater. Chem. A* **2013**, *1*, 4925−4936.
(24) Santana, R. P.; de Oliveira, N. A.; von Ranke, P. J. Magnetocaloric properties of compounds with first-order phase transition: Hysteresis effect. *J. Alloys Compd.* **2011**, *509*, 6346−6349.
(25) Miller, T. A.; Wittenberg, J. S.; Wen, H.; Connor, S.; Cui, Y.; Lindenberg, A. M. The mechanism of ultrafast structural switching in superionic copper (I) sulphide nanocrystals. *Nat. Commun.* **2013**, *4*, 1369−7.
(26) Makiura, R.; Yonemura, T.; Yamada, T.; Yamauchi, M.; Ikeda, R.; Kitagawa, H.; Kato, K.; Takata, M. Size-controlled stabilization of the superionic phase to room temperature in polymer-coated AgI nanoparticles. *Nat. Mater.* **2009**, *8*, 476−480.
(27) Schröter, W.; Nolting, J. Specific heats of crystals with the fluorite structure. *J. Phys. Colloques* **1980**, *41*, 20−23.
(28) Hull, S.; Berastegui, P.; Eriksson, S. G.; Gardner, N. J. G. Crystal structure and superionic conductivity of $PbF_2$ doped with KF. *J. Phys.: Condens. Matter* **1998**, *10*, 8429−8446.
(29) Walker, A. B.; Dixon, M.; Gillan, M. J. Computer simulation of ionic disorder in high-temperature $PbF_2$. *J. Phys. C: Solid State Phys.* **1982**, *15*, 4061−4073.
(30) Singh, S.; Fitzsimmons, M. R.; Lookman, T.; Jeen, H.; Biswas, A.; Roldan, M. A.; Varela, M. Role of elastic bending stress on magnetism of a Manganite thin film studied by polarized neutron reflectometry. *Phys. Rev. B: Condens. Matter Mater. Phys.* **2012**, *85*, 214440−6.
(31) Tosado, J.; Dhakal, T.; Biswas, A. Colossal piezoresistance in phase separated manganites. *J. Phys.: Condens. Matter* **2009**, *21*, 192203−3.
(32) Thiele, C.; Dörr, K.; Fähler, S.; Schultz, L.; Meyer, D. C.; Levin, A. A.; Paufler, P. Voltage-controlled epitaxial strain in films. *Appl. Phys. Lett.* **2005**, *87*, 262502−3.
(33) Plimpton, S. J. Fast Parallel Algorithms for Short-Range Molecular Dynamics. *J. Comput. Phys.* **1995**, *117*, 1−19.
(34) Kresse, G.; Furthmüller, J. Efficient iterative schemes for ab initio total-energy calculations using a plane-wave basis set. *Phys. Rev. B: Condens. Matter Mater. Phys.* **1996**, *54*, 11169−11185.
(35) Perdew, J. P.; Burke, K.; Ernzerhof, M. Generalized Gradient Approximation Made Simple. *Phys. Rev. Lett.* **1996**, *77*, 3865−3868.
(36) Blöchl, P. E. Projector augmented-wave method. *Phys. Rev. B: Condens. Matter Mater. Phys.* **1994**, *50*, 17953−17979.



DOI: 10.1021/acs.nanolett.6b00422
*Nano Lett.* 2016, 16, 3124−3129